J Nanostruct 16(4): 5806-5814, Autumn 2026

RESEARCH PAPER

Antimicrobial Resistance, Biofilm Formation, and the In Vitro Potential of Selenium–Antibiotic Nanoconjugates in *Pseudomonas aeruginosa* Bloodstream Isolates from Baghdad, Iraq

Ammar Khalid Shihab [1,2] *, ***Anas Y. Al-Hayawi*** [2]

[1] *Al-Dour Technical Institute, Northern Technical University, Al-Dour, Salahaddin, Iraq*

[2] *Biology Department, College of Education for Pure Sciences, Tikrit University, Tikrit, Iraq*

ARTICLE INFO

Article History:
Received 13 June 2026
Accepted 21 September 2026
Published 01 October 2026

Keywords:
Biofilm
Bloodstream
Nanoconjugates
Nanoparticles
P. aeruginosa
Selenium

ABSTRACT

Pseudomonas aeruginosa is a major cause of bloodstream infection in sepsis, and multidrug resistance and biofilm formation are increasingly making it difficult to treat. This study included 410 adult sepsis patients in Baghdad Specialized Teaching Hospital from January to March 2026. Blood cultures were processed using the BACT/ALERT 3D, and isolates were identified by VITEK 2 and by *rpoD* PCR. Susceptibility to 11 agents was tested using VITEK 2. Resistance was classified as MDR, XDR or PDR. Biofilm formation was assessed using the crystal violet assay. Selenium-amikacin, selenium-ciprofloxacin, and selenium-ceftazidime conjugates were prepared by selenite reduction and characterized by UV-Vis, FTIR, zeta potential, AFM and FESEM-EDS. MICs were determined by broth microdilution against four highly resistant isolates, and treated biofilms were analyzed by FE-SEM. Among 410 patients, 179 (43.7%) had positive blood cultures, yielding 31 P. aeruginosa isolates (17.3% of positive cultures). *P. aeruginosa* isolates showed the highest resistance to ciprofloxacin (77.4%), followed by ceftazidime (58.1%) and ceftolozane/tazobactam (54.8%). Overall, 71.0% of isolates were MDR, XDR, or possible PDR, while 85.2% of tested isolates formed biofilms. Selenium-antibiotic conjugate MICs ranged from 0.5 to 256 µg/mL, with activity varying by isolate and conjugate; free SeNPs showed no growth inhibition at concentrations up to 512 µg/mL. FE-SEM revealed biofilm disruption and cell filamentation. Bloodstream *P. aeruginosa* isolates showed high rates of multidrug resistance and biofilm formation. Selenium–antibiotic conjugates inhibited highly resistant isolates in an isolate-dependent manner, including a possible PDR isolate, and altered biofilm morphology. Future studies should quantify antibiotic loading and include concurrent free-drug controls.

How to cite this article
Khalid Shihab A, Al-Hayawi A. Antimicrobial Resistance, Biofilm Formation, and the In Vitro Potential of Selenium–Antibiotic Nanoconjugates in Pseudomonas aeruginosa Bloodstream Isolates from Baghdad, Iraq. J Nanostruct, 2026; 16(4):5806-5814.
DOI: 10.22052/JNS.2026.04.109

* *Corresponding Author Email: ammar.khalid@ntu.edu.iq*

This work is licensed under the Creative Commons Attribution 4.0 International License.
To view a copy of this license, visit http://creativecommons.org/licenses/by/4.0/.

INTRODUCTION

Sepsis remains one of the leading causes of morbidity and mortality worldwide [1]. Bacterial antimicrobial resistance caused an estimated 4.95 million deaths in 2019, with 1.27 million directly attributed to resistance [2]. *Pseudomonas aeruginosa* is a common and occasionally fatal cause of bloodstream infection (BSI) in critically ill patients [3]. Carbapenems and polymyxins are often the only remaining options because multidrug-resistant (MDR), extensively drug-resistant (XDR), and pandrug-resistant (PDR) phenotypes are spreading [4], and these can also fail [5].

Biofilm formation further complicates treatment. The extracellular polymeric substance (EPS) matrix hinders antibiotic diffusion, promotes metabolic dormancy and protects bacteria from phagocytosis [6]. Biofilm cells can withstand antimicrobial concentrations 1,000-fold higher than those that kill planktonic cells, contributing to treatment failure and persistent bacteremia [7]. Approaches that can breach these barriers are therefore needed [8].

Researchers are investigating selenium nanoparticles (SeNPs) as drug carriers and synergistic agents because of their physicochemical properties, biocompatibility, and intrinsic antibacterial activity [9], and hybrid selenium–antibiotic formulations may enhance activity against resistant and biofilm-associated bacteria [10]. The present study set out to determine the frequency, resistance patterns and biofilm-forming ability of *P. aeruginosa* in adult sepsis patients in Baghdad. Selenium conjugates of ceftazidime, amikacin and ciprofloxacin were then synthesised and characterised, and their minimum inhibitory concentrations and effects on biofilm structure were assessed in highly resistant bloodstream isolates.

MATERIALS AND METHODS

Study design

This cross-sectional study was performed in the internal medicine ward of Baghdad Specialized Teaching Hospital from January to March 2026. Four hundred and ten adults aged 18–55 years (267 males, 65.1%; 143 females, 34.9%) with sepsis as defined by Sepsis-3 (suspected infection plus an acute increase in SOFA score of ≥2) were enrolled. The age limit was chosen to prevent confounding by immunosenescence; comorbidities, immune status and prior antibiotic use were not exclusion criteria. Only the first non-contaminant isolate from each patient was studied. Proportions are presented with 95% confidence intervals

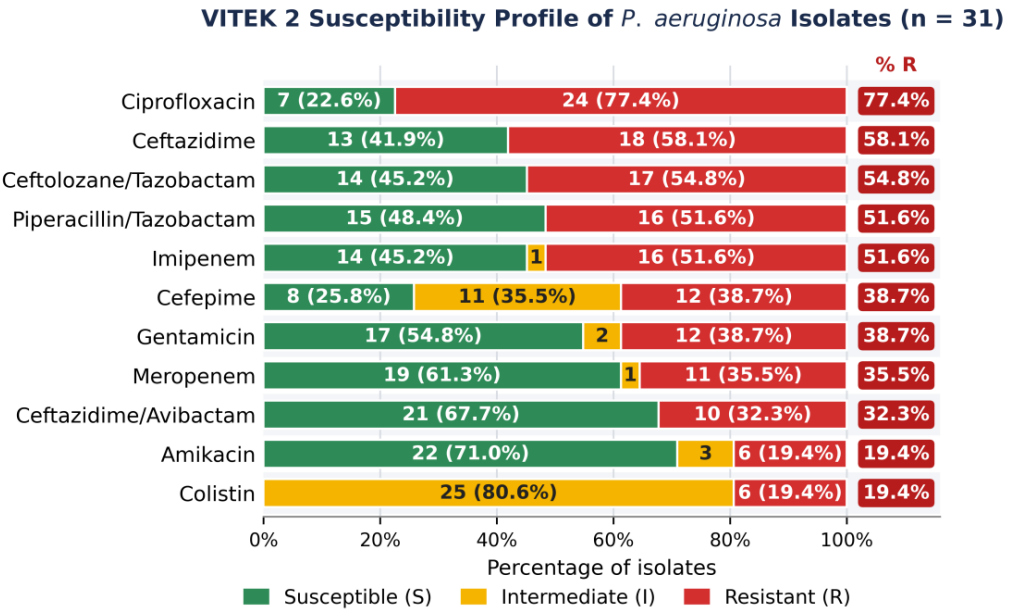


Fig. 1. Percentages of susceptible, intermediate and resistant results (%) for each antimicrobial agent among the 31 isolates of *P. aeruginosa*.

CC BY

calculated using the Wilson score method.

Identification and Susceptibility testing

Blood was inoculated into BACT/ALERT bottles containing resin and monitored on the BACT/ALERT 3D system. Positive bottles were subcultured onto Cetrimide agar (37 °C, 24–48 h). Isolates were identified using the VITEK 2 GN card (bioMérieux, France) and confirmed at genus level by *rpoD* PCR (primers PsEG30F/PsEG790R, ~760 bp; Mulet et al., 2009). Ten randomly selected isolates were identified to species level using the BioFire FilmArray BCID2 panel. Using VITEK 2 AST-N419 cards, susceptibility to 11 agents was determined and interpreted according to CLSI M100, 36th edition (CLSI, 2026). Isolates were classified as MDR, XDR or PDR according to [4]. Of the eight proposed categories of antimicrobials for *P. aeruginosa*, six were tested (monobactams and phosphonic acids were not), and colistin was tested with VITEK 2. The XDR and PDR assignments therefore correspond to the 'possible XDR' and 'possible PDR' categories of that proposal, and the terms XDR and PDR are used in this sense throughout. Intermediate results were counted as non-susceptible, except for colistin: CLSI M100 has no susceptible category for this agent, so an MIC ≤2 µg/mL (intermediate) was considered wild type and only MIC ≥4 µg/mL was counted as non-susceptible. Full protocols are described in the Supplementary Material.

Biofilm formation assay

Biofilm formation was assessed by the crystal violet microtiter-plate assay in tryptic soy broth (0.5 McFarland; 24 h static incubation at 37 °C; staining with 0.1% crystal violet; solubilization in 30% acetic acid; absorbance at 580 nm). Twenty-seven of the 31 isolates remained viable and were tested; four were lost during subculture. Each isolate was tested in triplicate wells, with sterile broth used as the negative control. The cutoff (ODc) was the negative control mean optical density plus three standard deviations. Isolates were categorised as non-adherent (OD ≤ ODc), weak (≤2 × ODc), moderate (≤4 × ODc) or strong (>4 × ODc) biofilm producers [11].

Synthesis and characterisation of selenium–antibiotic conjugates

Each conjugate (Se-ceftazidime, Se-amikacin, Se-ciprofloxacin) was prepared by adding 10 mL of antibiotic solution to 90 mL of 5 mM sodium selenite, stirring at 300 rpm for 1 h at room temperature, then incubating at 37 °C for 24 h. The yellow-to-brick-red change indicated reduction of selenite to elemental selenium, which is thought to be mediated by antibiotic functional groups (e.g., amine and hydroxyl groups) during incubation at 37 °C. The particles were collected by centrifugation at 10,000 rpm for 15 min, washed three times with deionized water and dried overnight at 40 °C. The yield was not determined. Bare SeNPs were prepared separately by dropwise addition of 10 mL of 50 mM ascorbic acid to 90 mL of 10 mM sodium selenite (500 rpm, 2 h, room temperature) and washed similarly. There was no quantification of antibiotic loading. The feed ratios were roughly

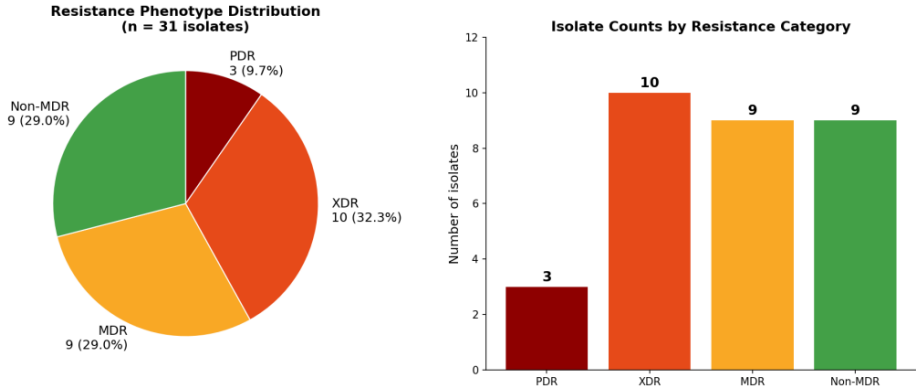


Fig. 2. Distribution of *P. aeruginosa* isolates according to resistance phenotype (n = 31). Left, proportions; right, numbers per category. XDR and PDR refer to the 'possible XDR' and 'possible PDR' categories of Magiorakos et al. (2012) (see Methods).

CC BY

2%, 10%, and 25% by mass for ciprofloxacin, ceftazidime, and amikacin, respectively, and all MICs are reported per total formulation mass. The conjugates were characterized by UV-Vis spectroscopy (200–700 nm), FTIR (4000–400 cm^{-1}), zeta potential (Brookhaven instrument, Smoluchowski model), atomic force microscopy (Nanosurf FlexAFM, static force mode, 2.5 × 2.5 µm scans; areal roughness Sa and Sq) and FESEM with energy-dispersive X-ray spectroscopy (EDS).

MIC determination

MICs were determined by broth microdilution in 96-well plates with two-fold dilutions in cation-adjusted Mueller–Hinton broth. The stock concentration was 1024 µg/mL for Se-ceftazidime and Se-amikacin and 256 µg/mL for Se-ciprofloxacin; the first well contained half the stock. Wells were inoculated with approximately 5 × 10^5 CFU/mL and incubated at 35 ± 2 °C for 20 h, with growth and sterility controls on every plate. Four highly resistant isolates were purposely selected to represent the most resistant phenotypes in the collection: the possible-PDR Isolate 4, Isolates 1 and 2 (XDR) and Isolate 5 (MDR). Isolate 3 was excluded due to inconsistent growth during sequential subculture, which would have compromised the reproducibility of the MIC assay. Free SeNPs were similarly assayed up to 512 µg/mL in separate plates. Colour controls (conjugate without bacteria) were included on all plates. Bacterial viability was read after addition of 20 µL of 0.015% resazurin. The lowest concentration without a pink colour shift was the MIC, and the value obtained in three independent runs was recorded.

FE-SEM analysis of treated biofilms

Isolate 4 biofilms were developed on sterile glass coverslips in 24-well plates with tryptic soy broth (0.5 McFarland, 37 °C, 24 h). Mature biofilms were then treated with bare SeNPs or individual conjugates at their respective MICs for 24 h. Controls were untreated samples. After washing, coverslips were fixed in 2.5% glutaraldehyde at 4 °C for 4 h and dehydrated in a series of ethanol concentrations (30–100%). The structural changes of the biofilms were observed by FE-SEM at 10 kV after air-drying and gold coating.

RESULTS AND DISCUSSION

Isolation and antimicrobial resistance

Blood cultures were positive in 179 out of 410 patients (43.7%). Of these, 34 (19%) grew on Cetrimide agar, and VITEK 2 profiling, supported by genus-level *rpoD* PCR, identified 31 isolates

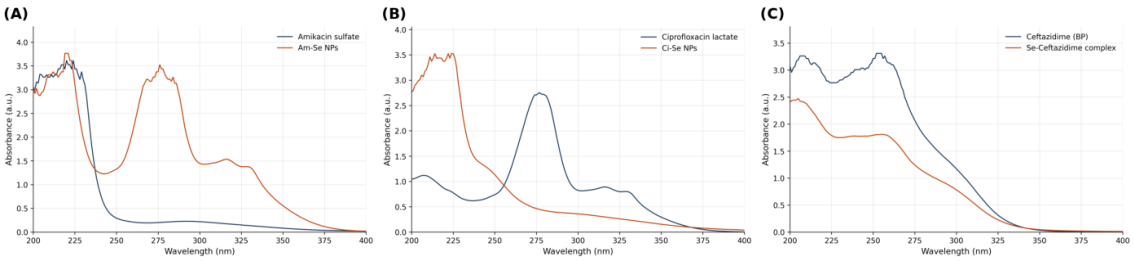


Fig. 3. UV-Vis absorption spectra (200–400 nm) of (A) amikacin sulfate and the Se-amikacin conjugate, (B) ciprofloxacin lactate and the Se-ciprofloxacin conjugate and (C) ceftazidime and the Se-ceftazidime conjugate. Legends in the spectra (Am-Se NPs, Ci-Se NPs, Se-Ceftazidime complex) refer to the Se-amikacin, Se-ciprofloxacin and Se-ceftazidime conjugates, respectively.

Table 1. Characterization of the selenium–antibiotic conjugates.

Conjugate	UV-Vis change	Zeta potential (mV)	AFM Sa / Sq (nm)	FESEM grain size (nm)	Se (atomic %)
Se-amikacin	Broad absorption at ~255–300 nm	+15.28	2.36 / 3.92	82–103	1.0–1.7
Se-ciprofloxacin	277 nm band no longer detected	+13.78	8.06 / 13.13	117–213	14.3–19.1
Se-ceftazidime	253 nm band reduced and broadened	−22.20	4.75 / 6.95	37–48	10.8–11.6

CC BY

as *P. aeruginosa* (17.3% of positive cultures and 7.6% of the whole cohort). Species-level identification was confirmed for 10 randomly selected isolates using the BioFire FilmArray BCID2 panel (10/10 agreement). Ciprofloxacin showed the most frequent resistance (77.4%), followed by ceftazidime (58.1%) and ceftolozane/tazobactam (54.8%), then piperacillin/tazobactam and imipenem (51.6% each), cefepime and gentamicin (38.7% each), meropenem (35.5%) and ceftazidime/avibactam (32.3%). Amikacin and colistin showed the lowest resistance (19.4% each), and 71.0% of isolates were susceptible to amikacin (Fig. 1). Three isolates (9.7%; 95% CI 3.3–24.9%) were PDR, 10 (32.3%) were XDR and 9 (29.0%) were MDR, so 22 of 31 isolates (71.0%; 95% CI 53.4–83.9%) fell into one of these categories and 9 (29.0%) were non-MDR (Fig. 2). PDR status applies to the antibiotics tested here. The VITEK 2 colistin results have not yet been confirmed by broth microdilution.

Biofilm formation

Of the 27 isolates tested, 23 (85.2%; 95% CI 67.5–94.1%) formed biofilm, of which 14 were strong, 4 moderate and 5 weak producers, and 4 isolates (14.8%) were non-adherent. Biofilm formation was common in MDR, XDR, and PDR isolates, but the sample size was too small to test for an association.

Characterization of the selenium–antibiotic conjugates

In the presence of each antibiotic, selenite reduction turned the mixture from yellow to brick-red. Conjugation altered the UV-Vis spectra (Fig. 3). Se-amikacin showed strong, broad absorption at about 255–300 nm, which was missing from amikacin sulfate (bands at 204–224 nm). The ciprofloxacin band at 277 nm was not detectable in Se-ciprofloxacin, and the ceftazidime band at 253 nm was reduced and broadened into a shoulder in Se-ceftazidime. Regions above 3 a.u. were out of the linear range and were not interpreted. The loss of the 277 nm ciprofloxacin band, which is in the linear range, is consistent with drug–selenium interaction, but low drug loading could also play a role. FTIR spectra showed that the main functional groups of each antibiotic were preserved and that bands were shifted, suggesting binding to selenium through hydroxyl and amine groups (amikacin), carboxylate and amide groups (ceftazidime, where the β-lactam C=O band remained at 1768.72 cm^{-1}) and carboxyl and keto groups (ciprofloxacin, where the carboxylic C=O band at 1726.29 cm^{-1} was no longer present). The Supplementary Material provides detailed band assignments. The zeta potentials were +15.28 mV for Se-amikacin, +13.78 mV for Se-ciprofloxacin and −22.20 mV for Se-ceftazidime, which fall within ±30 mV, suggesting moderate colloidal stability. AFM roughness (Sa) was 2.36 nm for Se-amikacin, 4.75 nm for Se-ceftazidime and 8.06 nm for Se-ciprofloxacin. FESEM revealed densely packed grains forming continuous films, and EDS confirmed selenium in all three conjugates (Table 1). The high sodium signal (7.2–24.1 atomic %) is likely to come from residual precursor or other sodium salts, and the trace nickel from instrumental background or the sample stub.

MICs of the conjugates

The MICs of the three conjugates against the four highly resistant isolates ranged from 0.5–256 µg/mL and varied by isolate and conjugate (Table 2). Se-ciprofloxacin was the most active (0.5–32 µg/mL), and the lowest MIC (0.5 µg/mL) was observed against the possible PDR isolate 4. Se-ceftazidime

Table 2. MICs (µg/mL) of the selenium–antibiotic conjugates against four highly resistant clinical isolates.

Isolate	Se-ceftazidime	Se-amikacin	Se-ciprofloxacin
Stock concentration	1024	1024	256
Free antibiotic (VITEK 2 MIC, reference only)	≥64	≥64	≥4
1	128	256	32
2	128	8	2
4 (possible PDR)	2	128	0.5
5	64	256	16

Note: Free-antibiotic MICs (VITEK 2) are provided for reference only; direct numerical comparison with conjugate MICs is not possible. Conjugate MICs refer to the total mass of the formulation (selenium plus conjugated antibiotic), and the S/I/R categories do not apply to nanoconjugates.

CC BY

inhibited this isolate at 2 µg/mL, compared with 64–128 µg/mL for the other isolates. Se-amikacin had the highest activity against Isolate 2 (8 µg/mL, versus 128–256 µg/mL for the others). The corresponding free antibiotics had VITEK 2 MICs of ≥64 µg/mL for ceftazidime, ≥64 µg/mL for amikacin and ≥4 µg/mL for ciprofloxacin. Free SeNPs did not inhibit any isolate at up to 512 µg/mL. These comparisons are only approximate: the free-antibiotic MICs are produced by an automated system and are censored at the upper limit of the cards, whereas the conjugate MICs are based on the total formulation mass. Because free SeNPs were inactive at the highest concentration tested, conjugate activity appears to depend on the antibiotic component, although it is not possible to quantify its contribution without loading data. Isolate 4, despite its possible PDR phenotype, was most susceptible to Se-ciprofloxacin and Se-ceftazidime; reference broth microdilution of the free antibiotics against the same isolate should confirm this.

Effect of the conjugates on biofilm morphology (FE-SEM)

Untreated biofilms of Isolate 4 were dense, continuous and multilayered, containing intact rod-shaped cells (width approximately 0.71–0.77 µm) immersed within a smooth EPS matrix (Fig. 4A). The treated biofilms differed from the control to varying extents (Fig. 4B–E). With bare SeNPs, the surface was fractured and blistered, with cells (approximately 0.90–1.07 µm wide) attached to surface aggregates. With Se-ciprofloxacin, cells had rough surfaces (about 0.54–0.73 µm wide), and the biofilm was less dense. Se-amikacin-treated biofilms showed thin, short or twisted cells (about 0.57–0.99 µm) with gaps and irregular areas, indicating a heterogeneous architecture [12]. The most obvious change was seen with Se-ceftazidime, where the multilayered biofilm was replaced by isolated cells or loose clusters of long filaments (>10 µm) on a largely uncovered substrate, with spherical nano-granules (around 22–25 nm) on the surface. The minor cracks seen in the control and bare SeNP samples likely reflect air-drying during preparation, while the long filaments and loss of biofilm structure seen only with Se-ceftazidime are treatment effects. These observations are qualitative and based on a single isolate.

The 43.7% blood-culture positivity is lower than

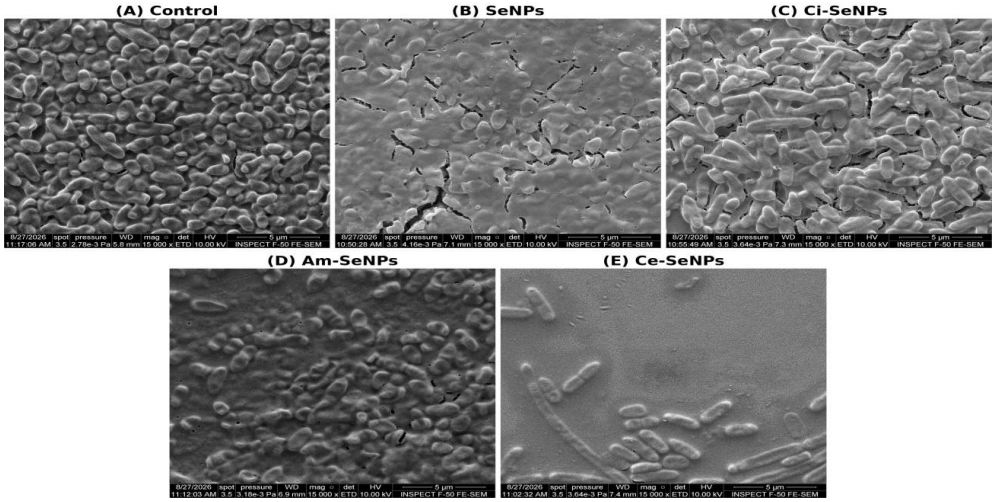


Fig. 4. Field Emission Scanning Electron Microscopy (FE-SEM) micrographs showing the structural and morphological changes in *Pseudomonas aeruginosa* biofilms. (A) Untreated control showing dense and continuous multilayered architecture with regular rod-shaped cells embedded in an intact EPS matrix. (B) Bare SeNPs, with fractured matrix and minor cellular blistering; (C) Se-ciprofloxacin, with rough-surfaced cells in a less dense network; (D) Se-amikacin, showing thin, short and twisted cell morphologies; and (E) Se-ceftazidime, displaying extreme cell filamentation (>10 µm) and biofilm structural collapse with sparse substrate coverage. Images were taken at 15,000× magnification (scale bars = 5 µm) at an accelerating voltage of 10 kV. Note: Ci-SeNPs, Am-SeNPs and Ce-SeNPs in the micrographs denote the Se-ciprofloxacin, Se-amikacin and Se-ceftazidime conjugates, respectively; SeNPs denotes bare selenium nanoparticles.

CC BY

the 70.3% reported for patients with suspected septicemia in Erbil [13], but higher than that typically reported in Western healthcare settings (20–30%) [14]. The 17.3% share of *P. aeruginosa* among positive cultures aligns with its established role as a leading nosocomial BSI pathogen [3]. Out of the 34 isolates that grew on Cetrimide agar, 31 were confirmed as *P. aeruginosa*, while the remaining three were *P. fluorescens* (n = 2) and *P. putida* (n = 1). This suggests that selective media can also support growth of related non-fermenters and that molecular confirmation is needed [15].

Resistance was common. Overall, 71.0% of isolates were MDR, XDR, or PDR, and XDR and PDR combined (41.9%) outnumbered MDR alone. The high resistance to ciprofloxacin (77.4%) is in accordance with the presence of *gyrA/parC* mutations and efflux overexpression (Qin et al., 2022). AmpC derepression, acquired β-lactamases and MexAB-OprM overexpression are widely reported as mechanisms of ceftazidime (58.1%) and piperacillin/tazobactam (51.6%) resistance, and 54.8% of isolates were non-susceptible to at least one carbapenem. The 12 isolates non-susceptible to both carbapenems may carry carbapenemases, whereas the five non-susceptible to imipenem but susceptible to meropenem show the phenotype usually associated with OprD loss. Likewise, the ten isolates resistant to both ceftolozane/tazobactam and ceftazidime/avibactam are consistent with metallo-β-lactamase production. These mechanisms are inferred from phenotype only and need molecular confirmation [2]. Amikacin was the most active agent (71.0% susceptible), and the higher gentamicin resistance aligns with aminoglycoside-modifying enzymes [2]. Colistin resistance (19.4%), including three PDR isolates, is worrisome because few options remain [2,5], but the VITEK 2 result should be confirmed by broth microdilution. The nine non-MDR isolates are a reminder that some infections still respond to standard agents, which is why susceptibility testing remains essential.

The high prevalence of biofilm formation (85.2%), along with widespread resistance, is clinically relevant. The EPS matrix hinders antibiotic access, induces dormancy in deeper layers, and protects cells from host defences [16]; biofilm cells can also survive up to 1,000-fold higher antibiotic concentrations [6]. This supports the search for anti-biofilm strategies such as nano-conjugated delivery systems.

The UV-Vis changes (broad absorption at ~255–300 nm for Se-amikacin, loss of the 277 nm ciprofloxacin band, and attenuation of the 253 nm ceftazidime band) suggest altered chromophore environments, consistent with interactions between the drugs and the selenium surface [9]. The FTIR shifts suggest involvement of hydroxyl/amine, carboxyl/keto, and carboxylate/amide groups, and that the β-lactam ring of ceftazidime remained intact. Zeta potentials indicated moderate colloidal stability. The lower selenium content of Se-amikacin and the high sodium signal indicate that loading differs between conjugates and that purification was incomplete.

The conjugates inhibited the four resistant isolates in an isolate- and conjugate-dependent way, while free SeNPs were inactive at up to 512 µg/mL. The low MICs, especially for Se-ciprofloxacin, suggest that the formulation has an enhanced inhibitory effect dependent on the antibiotic component. The selenium core may help deliver the drug to the cell envelope or induce local membrane damage. HPLC quantification of drug loading and checkerboard (FICI) assays will be needed to determine whether this effect is synergistic. Variation between isolates may reflect intrinsic mechanisms such as efflux or porin changes. A “Trojan horse” mechanism, in which the antibiotic anchors the particle to the cell envelope and the SeNP core protects the drug while generating reactive oxygen species (ROS), is plausible but untested here. SeNPs have been reported to deplete ATP, destabilize membrane potential and induce oxidative stress [17], to show antibacterial and antibiofilm activity against *P. aeruginosa* [18] and to interfere with LasI/R and RhlI/R quorum-sensing regulators, according to docking studies [19].

The FE-SEM morphologies match the known modes of action of the antibiotics. Classical inhibition of gyrase and topoisomerase IV arrests cell division and induces filamentation [20,21], but the changes in cell dimensions seen with Se-ciprofloxacin (Fig. 4C) require quantitative measurements of cell length and width before interpretation. The extensive filamentation (>10 µm) with Se-ceftazidime is characteristic of PBP3 inhibition and blocked septum formation [22], and the loosely arranged filaments without surrounding EPS suggest that the transition from attachment to mature biofilm was blocked [23]. The thin, twisted cells observed with Se-amikacin are consistent

CC BY

with the incorporation of mistranslated proteins into the membrane following binding to the 30S ribosomal subunit [24]. Amikacin–SeNP conjugates have been reported to improve antibacterial and antibiofilm activity [25].

Overall, the findings link a clinical problem with a candidate approach. Seven out of ten bloodstream isolates were MDR, XDR, or PDR, and 85.2% of those tested formed biofilms, so treatment options are limited, and biofilm tolerance may further narrow them. In this context, the conjugates inhibited highly resistant isolates, including a possible PDR isolate, at 0.5–2 µg/mL (Se-ciprofloxacin and Se-ceftazidime, Isolate 4), whereas free SeNPs were inactive. FE-SEM also showed morphological changes in a mature biofilm that planktonic MICs do not capture, most clearly with Se-ceftazidime. How this will translate into clinical benefit remains to be determined by quantifying antibiotic loading, concurrent broth-microdilution and checkerboard assays, larger isolate panels with replicate-based statistics, quantitative anti-biofilm assays and hemocompatibility testing.

This basic *in vitro* study provides preliminary qualitative evidence of the conjugates' effectiveness, but some limitations remain. First, susceptibility to colistin was determined with an automated system (VITEK 2) and still requires confirmation by broth microdilution in accordance with CLSI guidelines; hence, the extreme resistance phenotypes are reported as 'possible' according to [4]. Second, quantifying absolute drug-loading capacity (e.g., via HPLC) and calculating Fractional Inhibitory Concentration Indices (FICI) via checkerboard assays are critical next steps needed to determine whether the effect is synergistic before future *in vivo* translation. Antibiotic loading was not quantified, so fold changes cannot be calculated; free-antibiotic MICs were obtained with VITEK 2 and are censored, and conjugate MICs refer to total formulation mass. Free drugs, bare SeNPs, physical mixtures and conjugates were not examined on the same plates; no checkerboard assays were performed, and residual selenite could have contributed to inhibition. Hence, the results should be interpreted as a descriptive proof of concept. Only four isolates were tested for MIC, and one for FE-SEM, and the FE-SEM analysis was qualitative. Complementary techniques (UV-Vis, FTIR, zeta potential, AFM, and FE-SEM–EDS) supported conjugation, but crystallographic characterisation (XRD) and hydrodynamic characterisation (TEM and DLS) were not performed and are needed to define particle size and crystallinity. Moreover, some UV-Vis spectra were above the linear absorbance range and should be repeated on diluted suspensions, and the FE-SEM samples were air-dried, which can cause minor surface cracking. The study was also performed at a single centre; the cohort included patients aged 18–55 years, and comorbidities, immunosuppression, and prior antibiotic exposure were not controlled, so the epidemiological data may not represent older patients. Finally, the present study was devoted to antibacterial activity and qualitative effects on biofilm structure. A separate evaluation has addressed the *in vitro* cytotoxicity of the conjugates, which indicated low toxicity (unpublished data); these results will be reported in a separate manuscript together with gene expression and next-generation sequencing (NGS) analyses. Quantitative anti-biofilm and hemocompatibility assays are also planned.

CONCLUSION

Pseudomonas aeruginosa constituted 17.3% of positive blood cultures in adult sepsis patients; 71.0% of isolates were MDR, XDR, or possible PDR, and 85.2% formed biofilm. Amikacin, ciprofloxacin and ceftazidime selenium conjugates were synthesized and characterized, and they inhibited highly resistant isolates including a possible-PDR isolate (MIC 0.5–256 µg/mL) in an isolate- and conjugate-dependent manner, while free SeNPs were inactive. FE-SEM showed altered biofilm morphology, most prominently with Se-ceftazidime. These *in vitro* results justify further evaluation of selenium–antibiotic conjugates against highly resistant *P. aeruginosa* with concurrent controls, measured antibiotic loading and larger isolate panels.

CONFLICT OF INTEREST

The authors declare that there is no conflict of interests regarding the publication of this manuscript.

REFERENCES

1. Santacroce E, D'Angerio M, Ciobanu AL, Masini L, Lo Tartaro D, Coloretti I, et al. Advances and Challenges in Sepsis Management: Modern Tools and Future Directions. Cells. 2024;13(5):439.
2. Ranjbar R, Alam M. Antimicrobial Resistance Collaborators (2022). Global burden of bacterial antimicrobial resistance

CC BY

in 2019: a systematic analysis. Evidence Based Nursing. 2023;27(1):16-16.
3. Qin S, Xiao W, Zhou C, Pu Q, Deng X, Lan L, et al. Pseudomonas aeruginosa: pathogenesis, virulence factors, antibiotic resistance, interaction with host, technology advances and emerging therapeutics. Signal Transduction and Targeted Therapy. 2022;7(1).
4. Magiorakos AP, Srinivasan A, Carey RB, Carmeli Y, Falagas ME, Giske CG, et al. Multidrug-resistant, extensively drug-resistant and pandrug-resistant bacteria: an international expert proposal for interim standard definitions for acquired resistance. Clinical Microbiology and Infection. 2012;18(3):268-281.
5. Sole E, Trinchera M, De Gaetano S, Midiri A, Piccolo G, Mancuso G, et al. The Paradox of Healthcare in the 'Superbugs' Era: Current Challenges and Future Directions. Pathogens. 2025;14(12):1199.
6. Haidar A, Muazzam A, Nadeem A, Atique R, Saeed HA, Naveed A, et al. Biofilm formation and antibiotic resistance in Pseudomonas aeruginosa. The Microbe. 2024;3:100078.
7. Thöming JG, Häussler S. Pseudomonas aeruginosa Is More Tolerant Under Biofilm Than Under Planktonic Growth Conditions: A Multi-Isolate Survey. Frontiers in Cellular and Infection Microbiology. 2022;12.
8. Farah H, Kadhim-Abosaoda M, Mohaisen-Mousa H, Renuka Jyothi S, Priyadarshini-Nayak P, Bethanney Janney J, et al. Nanomedicine Strategies Against Biofilm-Associated Infections: Advances, Challenges, and Translational Barriers. MicrobiologyOpen. 2025;15(1).
9. Satpathy S, Samal P, Panigrahi LL, Pradhan AK, Arakha M. Biosynthesis of Selenium Nanoparticles Functionalized with Cetrimonium Bromide Exhibits Enhanced Antimicrobial Activity against Pathogenic Bacterial Strains and Effective Photoaccelerated Detoxification of Sulfamethoxazole. ACS Omega. 2026.
10. Han H-W, Patel KD, Kwak J-H, Jun S-K, Jang T-S, Lee S-H, et al. Selenium Nanoparticles as Candidates for Antibacterial Substitutes and Supplements against Multidrug-Resistant Bacteria. Biomolecules. 2021;11(7):1028.
11. StepanoviĆ S, VukoviĆ D, Hola V, Bonaventura GD, DjukiĆ S, ĆirkoviĆ I, et al. Quantification of biofilm in microtiter plates: overview of testing conditions and practical recommendations for assessment of biofilm production by staphylococci. APMIS. 2007;115(8):891-899.
12. Flemming H-C, van Hullebusch ED, Neu TR, Nielsen PH, Seviour T, Stoodley P, et al. The biofilm matrix: multitasking in a shared space. Nature Reviews Microbiology. 2022;21(2):70-86.
13. Aka STH. Surveillance of multidrug-resistant bacterial isolates from bloodstream infections in Erbil, Iraq. The Journal of Infection in Developing Countries. 2026;20(05):670-677.
14. Lamy B, Dargère S, Arendrup MC, Parienti J-J, Tattevin P. How to Optimize the Use of Blood Cultures for the Diagnosis of Bloodstream Infections? A State-of-the Art. Front Microbiol. 2016;7.
15. Mulet M, Bennasar A, Lalucat J, García-Valdés E. An rpoD-based PCR procedure for the identification of Pseudomonas species and for their detection in environmental samples. Molecular and Cellular Probes. 2009;23(3-4):140-147.
16. Fernández-Billón M, Llambías-Cabot AE, Jordana-Lluch E, Oliver A, Macià MD. Mechanisms of antibiotic resistance in Pseudomonas aeruginosa biofilms. Biofilm. 2023;5:100129.
17. Huang T, Holden JA, Heath DE, O'Brien-Simpson NM, O'Connor AJ. Engineering highly effective antimicrobial selenium nanoparticles through control of particle size. Nanoscale. 2019;11(31):14937-14951.
18. Thamayandhi C, El-Tayeb MA, Syed SRM, Sivaramakrishnan R, Gunasekar B. Antibacterial and anti-biofilm efficacy of selenium nanoparticles against Pseudomonas aeruginosa: Characterization and in vitro analysis. Microb Pathog. 2024;196:106998.
19. Kanak KR, Dass RS, Pan A. Anti-quorum sensing potential of selenium nanoparticles against LasI/R, RhlI/R, and PQS/MvfR in Pseudomonas aeruginosa: a molecular docking approach. Frontiers in Molecular Biosciences. 2023;10.
20. Bush NG, Diez-Santos I, Abbott LR, Maxwell A. Quinolones: Mechanism, Lethality and Their Contributions to Antibiotic Resistance. Molecules. 2020;25(23):5662.
21. Huynh TQ, Tran NBV, Pham TTV, Le VBT, Truong TP, Huynh VA, et al. Adaptive response of Pseudomonas aeruginosa under serial ciprofloxacin exposure. Microbiology. 2024;170(3).
22. Hayes MV, Orr DC. Mode of action of ceftazidime: affinity for the penicillin-binding proteins of Escherichia coli K12, Pseudomonas aeruginosa and Staphylococcus aureus. J Antimicrob Chemother. 1983;12(2):119-126.
23. Thi MTT, Wibowo D, Rehm BHA. Pseudomonas aeruginosa Biofilms. Int J Mol Sci. 2020;21(22):8671.
24. Davis BD. Mechanism of bactericidal action of aminoglycosides. Microbiol Rev. 1987;51(3):341-350.
25. Ridha DM, Al-Awady MJ, Abd Al-Zwaid AJ, Balakit AA, Al-Dahmoshi HOM, Alotaibi MH, et al. Antibacterial and antibiofilm activities of selenium nanoparticles-antibiotic conjugates against anti-multidrug-resistant bacteria. Int J Pharm. 2024;658:124214.

CC BY